

See discussions, stats, and author profiles for this publication at: <https://www.researchgate.net/publication/231719697>

Molecular analogs of surface species. 3. The mechanism of the regioselective homogeneous hydrogenation of benzothiophene by use of $[\text{Rh}(\text{COD})(\text{PPh}_3)_2]\text{PF}_6$ as the catalyst precursor. Ki...

ARTICLE in ORGANOMETALLICS · FEBRUARY 1994

Impact Factor: 4.13 · DOI: 10.1021/om00014a029

CITATIONS

34

READS

7

5 AUTHORS, INCLUDING:



Roberto Sánchez-Delgado

City University of New York - Brooklyn College

117 PUBLICATIONS 3,434 CITATIONS

SEE PROFILE



Luis Rincon

University of the Andes (Venezuela)

72 PUBLICATIONS 549 CITATIONS

SEE PROFILE

Molecular Analogues of Surface Species. 3. The Mechanism of the Regioselective Homogeneous Hydrogenation of Benzothiophene by Use of $[\text{Rh}(\text{COD})(\text{PPh}_3)_2]\text{PF}_6$ as the Catalyst Precursor. Kinetic and Theoretical Study

Roberto A. Sánchez-Delgado,* Verónica Herrera, Luis Rincón, Antida Andriollo, and Gonzalo Martín

Chemistry Center, Instituto Venezolano de Investigaciones Científicas (IVIC), Caracas 1020-A, Venezuela

Received October 18, 1993*

The mechanism of the regioselective hydrogenation of benzo[*b*]thiophene (BT) to 2,3-dihydrobenzo[*b*]thiophene (DHBT) in 2-methoxyethanol solution at 125 °C and ambient or subambient pressure of H_2 , using $[\text{Rh}(\text{COD})(\text{PPh}_3)_2]\text{PF}_6$ (1) (COD = 1,3-cyclooctadiene) as the catalyst precursor has been investigated by a combination of kinetic, chemical, and theoretical methods. The kinetic study led to a rate law $r_1 = k_7 K_6 [\text{Rh}]_0 [\text{H}_2] / (1 + K_6 [\text{H}_2])$, where $(k_{\text{cat}})_{\text{exp}} = k_7 K_6 = 0.726 \text{ M}^{-1} \text{ s}^{-1}$, $k_7 = 3.70 \times 10^{-2} \text{ s}^{-1}$, and $K_6 = 19.61 \text{ M}^{-1}$. The calculated activation parameters are $\Delta H^\ddagger = 20.1 \pm 0.9 \text{ kcal/mol}$, $\Delta S^\ddagger = -11.1 \pm 0.8 \text{ eu}$, and $\Delta G^\ddagger = 23 \pm 3 \text{ kcal/mol}$. 1 probably reacts with hydrogen to produce an unstable intermediate $[\text{RhH}_2(\eta^1\text{-S-BT})(\text{PPh}_3)_2]^+$ which evolves into $[\text{Rh}(\pi\text{-BT})(\text{PPh}_3)_2]^+$, where BT is likely to be η^5 -bonded through the thiophene ring. Semiempirical (CNDO) theoretical calculations on the interactions of the fragment $[\text{Rh}(\text{PPh}_3)_2]^+$ with BT revealed that both η^5 -bonding through the thiophene ring and η^6 -bonding through the benzene ring are possible; in the former case, the bonding is dominated by donation from a filled $5a'$ BT orbital localized mainly on the S lone pair to empty $3a_1$ and $2b_1$ metal orbitals, whereas in the latter the main interaction is donation from a delocalized $4a'$ BT orbital to an empty b_2 metal orbital. The dihydride $[\text{Rh}(\text{BT})(\text{H})_2(\text{PPh}_3)_2]^+$ which is formed by reaction of $[(\eta^5\text{-BT})\text{Rh}(\text{PPh}_3)_2]^+$ with H_2 may contain BT coordinated $\eta^1\text{-S}$, $\eta^2\text{-C}_2=\text{C}_3$, or η^4 ; $[\text{Rh}(\eta^4\text{-BT})(\text{H})_2(\text{PPh}_3)_2]^+$ was found to be more stable than $[\text{Rh}(\eta^1\text{-BT})(\text{H})_2(\text{PPh}_3)_2]^+$ and $[\text{Rh}(\eta^2\text{-BT})(\text{H})_2(\text{PPh}_3)_2]^+$. The largest activation of the C=C bond of the thiophene moiety is produced by the η^2 mode of bonding. All this information leads to a hydrogenation mechanism in which the active species is most probably the 18 electron π -bonded species $[\text{Rh}(\eta^5\text{-BT})(\text{PPh}_3)_2]^+$, which is in equilibrium with an olefin-like complex $[\text{Rh}(\text{H})_2(\eta^2\text{-BT})(\text{PPh}_3)_2]^+$. The rate determining step of the catalytic reaction is the transfer of hydrides from Rh to $\eta^2\text{-BT}$, to yield $[\text{Rh}(\eta^1\text{-S-DHBT})(\text{PPh}_3)_2]^+$; subsequent rapid reaction with BT liberates the product and restarts the catalytic cycle. This mechanism provides a good model for understanding the initial hydrogenation step in the heterogeneous hydrodesulfurization of BT on solid catalysts.

Introduction

The homogeneous hydrogenation of sulfur-containing aromatic compounds by transition metal complexes has received little attention. This reaction may be of great utility in synthetic applications and is certainly of interest in relation to the fundamental understanding of the mechanisms involved in the industrially important hydrodesulfurization (HDS) process.¹ Benzo[*b*]thiophene (BT) is a particularly interesting substrate, since it represents one of the most abundant and refractory classes of compounds present in heavy oils. One of the most widely accepted mechanisms proposed for HDS of BT over solid catalysts involves the selective hydrogenation to 2,3-dihydrobenzo[*b*]thiophene (DHBT) prior to desulfuriza-

tion to yield ethylbenzene.^{1f-g} Little is known, however, about the ways in which such hydrogenation of the thiophene moiety takes place.

We have previously reported that a number of Ru, Os, Rh, and Ir complexes catalyze the regioselective hydrogenation of N- and S-heterocycles, including BT to DHBT.² Fish and co-workers have published over the last several years extensive studies on the selective reduction of aromatic and nitrogen-heteroaromatic compounds catalyzed by a number metal complexes, particularly of Rh and Ru.³ Some aspects of the hydrogenation of BT to DHBT were also described in their publications, and a catalytic cycle for this transformation was recently

* Abstract published in *Advance ACS Abstracts*, December 15, 1993.

(1) (a) Schuman, S. C.; Shalit, H. *Catal. Rev.* 1970, 4, 245. (b) Mitchell, P. C. H. In *Catalysis*; Kemball, C., Ed.; The Chemical Society: London, 1977; Vol. 1, p 223; Vol. 4, p 203. (c) Gates, B. C.; Katzer, J. R.; Schuit, G. C. A. *Chemistry of Catalytic Processes*; McGraw-Hill: New York, 1979. (d) Grange, P. *Catal. Rev.-Sci. Eng.* 1980, 21, 135. (e) Wiegand, B. C.; Friend, C. M. *Chem. Rev.* 1992, 92, 491. (f) López, R.; Peter, D.; Zdravil, M. *Collect. Czech. Chem. Commun.* 1981, 46, 2185. (g) Girgis, M. J.; Gates, B. C. *Ind. Eng. Chem. Res.* 1991, 30, 2021.

(2) (a) Sánchez-Delgado, R. A.; González, E. *Polyhedron* 1989, 8, 1431. (b) Sanchez-Delgado, R. A. In *Advances in Catalyst Design*; Graziani, M.; Rao, C. N. R., Eds.; World Scientific Publishing Co.: Singapore, 1991; p 214.

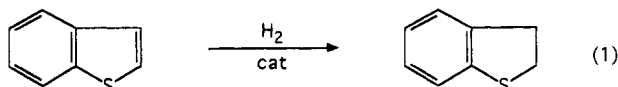
(3) (a) Fish, R. H.; Thormodsen, A. D.; Cremer, G. A. *J. Am. Chem. Soc.* 1982, 104, 5234. (b) Fish, R. H. *Ann. N.Y. Acad. Sci.* 1983, 415, 292. (c) Fish, R. H.; Tan, J. L.; Thormodsen, A. D. *J. Org. Chem.* 1984, 49, 4500. (d) Fish, R. H.; Tan, J. L.; Thormodsen, A. D. *Organometallics* 1985, 10, 1743. (e) Fish, R. H.; Baralt, E.; Smith, S. J. *Organometallics* 1991, 10, 54. (f) Baralt, E.; Smith, S. J.; Hurwitz, J.; Horváth, I.; Fish, R. H. *J. Am. Chem. Soc.* 1992, 114, 5187.

proposed.^{3f} The coordination and activation of sulfur heteroaromatics has also received a great deal of attention in recent times, both from an experimental and a theoretical point of view, as molecular analogues of surface species and interactions implicated in HDS.^{1d,2b,4,5}

The kinetic behavior of a homogeneous catalytic system is a key feature in the understanding of the reaction mechanism; such studies have been carried out for the hydrogenation of C=C,⁶ C≡C,⁷ C=O⁸ bonds and aromatic hydrocarbons,^{8a,9} but to our knowledge, there are no previous reports on the kinetics of homogeneous hydrogenation of heteroaromatic compounds, except for our own recent work on quinoline.^{2b,10} Theoretical calculations provide an additional powerful tool for establishing reaction mechanisms, but the number of such studies for homogeneous catalytic cycles is rather limited, and most of the attention has been devoted to C=C bond hydrogenation and metathesis.¹¹ In this paper we describe a kinetic and theoretical investigation of the mechanism of the homogeneous hydrogenation of BT using as the catalyst precursor the cationic rhodium complex [Rh(COD)-(PPh₃)₂]PF₆ (COD = 1,3-cyclooctadiene) (1), which we hope will contribute to a clear understanding of this important reaction.

Results and Discussion

The specific hydrogenation of BT to DHBT (eq 1) was carried out using 1 as the catalyst precursor in 2-methoxyethanol solution at 125 °C and ambient or subambient pressure.



The homogeneity of the hydrogenation runs was inferred from the high selectivity observed, together with an excellent reproducibility of the kinetic measurements, and from the fact that addition of mercury to the solutions did not affect the catalytic rates.¹²

Reaction Kinetics. The kinetics of the hydrogenation of BT to DHBT were studied by carrying out runs at different catalyst, substrate, and hydrogen concentrations

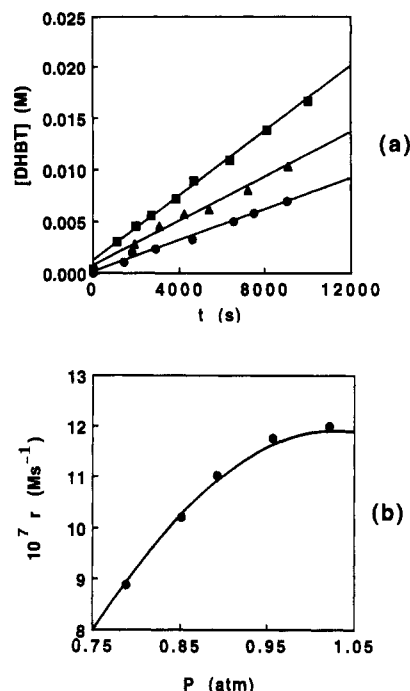


Figure 1. Hydrogenation of benzothiophene to 2,3-dihydrobenzothiophene by complex 1. (a) Examples of hydrogen uptake measurements at different catalyst concentrations: (●) 5.0×10^{-4} M; (▲) 6.5×10^{-4} M; (■) 10^{-3} M. [BT] = 5.0×10^{-2} M; [H₂] = 2.3×10^{-3} M; $T = 125$ °C; solvent, 2-methoxyethanol. (b) Rate dependence on H₂ concentration. Conditions are as in Table 1.

Table 1. Kinetic Data for the Hydrogenation of Benzothiophene^a with [Rh(COD)(PPh₃)₂]PF₆ as the Catalyst Precursor

$10^4[\text{Rh}]$ (M)	$10^2[\text{BT}]$ (M)	$10^3[\text{H}_2]$ (M)	$P(\text{H}_2)$ (mmHg)	T (°C)	$10^7 r_i$ (M s ⁻¹)
5.0	5.0	2.3	663.5	125	7.8
5.5	5.0	2.3	663.5	125	9.0
6.0	5.0	2.3	663.5	125	10.3
6.5	5.0	2.3	663.5	125	10.7
7.0	5.0	2.3	663.5	126	12.0
8.0	5.0	2.3	663.5	126	13.7
10.0	5.0	2.3	663.5	126	15.8
6.0	6.2	2.3	663.5	125	4.9
6.0	1.0	2.3	663.5	126	6.5
6.0	3.0	2.3	663.5	125	3.3
6.0	8.0	2.3	663.5	125	1.2
6.0	10.0	2.3	663.5	126	7.0
6.0	5.0	2.0	599.0	125	8.9
6.0	5.0	2.2	647.5	125	10.2
6.0	5.0	2.4	679.0	125	11.0
6.0	5.0	2.5	727.0	125	11.8
6.0	5.0	2.7	776.0	125	12.0
6.0	5.0	2.3	663.5	111	3.7
6.0	5.0	2.3	663.5	116	5.2
6.0	5.0	2.3	663.5	130	15.6

^a Solvent: 2-methoxyethanol (50 mL); r_i = initial rates.

and at different temperatures. Representative examples of catalytic runs are shown in Figure 1a, and the complete data are listed in Table 1.

The initial rates (r_i) showed a direct dependence with respect to the catalyst concentration. A plot of $\log r_i$ vs $\log [\text{Rh}]$ yielded a straight line of slope 1.00, which confirms

(4) (a) Angelici, R. J. *Acc. Chem. Res.* 1988, 21, 387. (b) Angelici, R. J. *Coord. Chem. Rev.* 1990, 105, 61. (c) Rauchfuss, T. B. *Prog. Inorg. Chem.* 1991, 39, 259. (d) Bianchini, C.; Meli, A.; Peruzzini, M.; Vizza, F.; Frediani, P.; Herrera, V.; Sánchez-Delgado, R. A. *J. Am. Chem. Soc.* 1993, 115, 2731.

(5) Ruetter, F.; Valencia, N.; Sánchez-Delgado, R. A. *J. Am. Chem. Soc.* 1989, 111, 40.

(6) (a) Halpern, J.; Wong, C. S. *J. Chem. Soc., Chem. Commun.* 1973, 629. (b) Halpern, J.; Okamoto, T.; Zakhariev, A. *J. Mol. Catal.* 1977, 2, 65. (c) Riley, D. P.; Chan, A. C. S.; Pluth, J. J. *J. Am. Chem. Soc.* 1977, 99, 8056. (d) Chan, A. C. S.; Halpern, J. *J. Am. Chem. Soc.* 1980, 102, 838. (e) Halpern, J. *Inorg. Chim. Acta* 1981, 50, 11. (f) Esteruelas, M. A.; Herrero, J.; López, A. M.; Oro, L. A.; Schulz, M.; Werner, H. *Inorg. Chem.* 1992, 31, 4013.

(7) (a) Andriollo, A.; Esteruelas, M. A.; Meyer, U.; Oro, L. A.; Sánchez-Delgado, R. A.; Sola, E.; Valero, C.; Werner, H. *J. Am. Chem. Soc.* 1989, 111, 7431-7437. (b) Esteruelas, M. A.; López, A. M.; Oro, L. A.; Perez, A.; Schultz, M.; Werner, H. *Organometallics* 1993, 12, 1823.

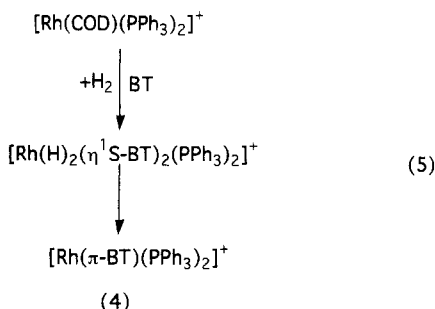
(8) (a) Halpern, J.; Linn, D. E. *J. Am. Chem. Soc.* 1987, 109, 2969. (b) Halpern, J. *Pure Appl. Chem.* 1987, 59, 173. (c) Rosales, M.; González, A.; Alvarado, Y.; Rubio, R.; Andriollo, A.; Sánchez-Delgado, R. *J. Mol. Catal.* 1992, 75, 1.

(9) (a) Landis, C. R.; Halpern, J. *Organometallics* 1983, 2, 840. (b) Halpern, J.; Fordyce, W. A.; Wilczynski, R. *J. Organomet. Chem.* 1985, 296, 115.

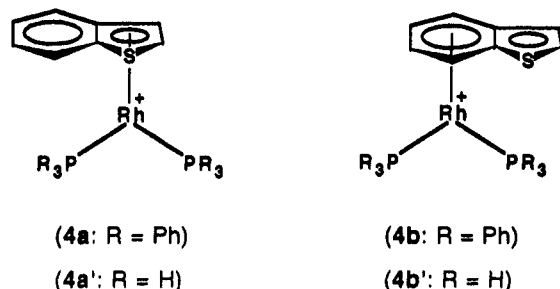
(10) Sánchez-Delgado, R. A.; Rondón, D.; Andriollo, A.; Martín, G.; Chaudret, B. *Organometallics* 1993, 12, 4291.

(11) Koga, N.; Morokuma, K. *Chem. Rev.* 1991, 91, 823 and references therein.

(12) (a) Crabtree, R.; Anton, D. R. *Organometallics* 1983, 2, 855. (b) Sánchez-Delgado, R. A.; Andriollo, A.; Puga, J.; Martín, G. *Inorg. Chem.* 1987, 26, 1867. (c) Whitesides, G. M.; Hacket, M.; Brainard, R. L.; Lavalleye, J.-P. P. M.; Sowinski, A. F.; Izumi, A. N.; Moore, S. S.; Brawn, D. W.; Staudt, E. M. *Organometallics* 1985, 4, 1819.



Our efforts to obtain this species in a pure form have so far proved unsuccessful, which has precluded a proper characterization. We have attempted additional *in situ* NMR experiments to help us elucidate the mode of bonding of BT to rhodium in 4, since both π -coordination through the thiophene ring (4a) or through the benzene



ring (4b) are possible. When hydrogen is bubbled through a CD_2Cl_2 solution of 1 in the presence of excess T, the resulting ^{31}P NMR spectrum consists of a doublet at 40.8 ppm ($J_{\text{Rh-P}} = 198$ Hz), corresponding to 3; if BT is used instead, the spectrum displays as the main feature a doublet at 40.0 ppm ($J_{\text{Rh-P}} = 112$ Hz). On the other hand, an analogous reaction carried out in the presence of naphthalene generates a doublet shifted to 36.8 ppm ($J_{\text{Rh-P}} = 192$ Hz), presumably due to $[\text{Rh}(\eta^6\text{-naphthalene})(\text{PPh}_3)_2]^+$; our attempts to isolate this arene complex have led to complex mixtures which are formed during workup. We note that the value of the chemical shift in the case of BT is closer to that observed for T than for naphthalene, but the opposite trend was found for the Rh-P coupling constants; therefore, these results are ambiguous concerning the mode of bonding of BT to rhodium.

Both the η^5 (4a) and the η^6 (4b) modes of bonding allow an 18-electron configuration to be achieved. The η^5 -coordination mode is now well documented for metal-thiophene complexes^{4,14} but has no precedent in the case of metal-BT derivatives; all the stable BT complexes reported so far have been shown to be π -coordinated through the benzene ring to the metal.^{4c} However, the following literature precedents indicate that the η^5 rather than that the η^6 form is implicated in our hydrogenation catalysis: (i) it has been shown that hydride attack to η^6 -BT Ru and Ir complexes occurs exclusively at the 7-position and never to the thiophene ring, as a result of the activation caused by coordination of the benzene ring;¹⁸ (ii) H-D exchange in $[\text{CpRu}(\eta^6\text{-BT})]^+$ takes place only at the 2- and 7-positions, whereas on heterogeneous HDS catalysts H-D exchange occurs selectively at the 2- and 3-positions. This was taken by Angelici and co-workers

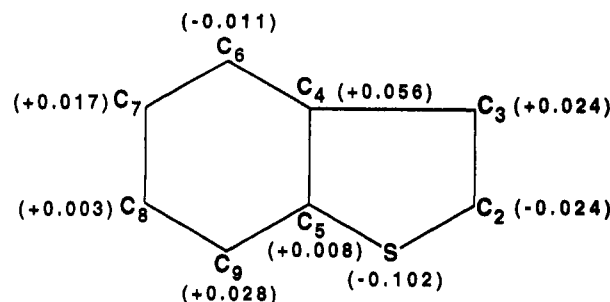


Figure 3. Charge on the atoms in BT.

as suggestive that the π -benzene type of coordination does not activate BT toward hydrogenation or hydrogenolysis of the thiophenic ring, and that a small equilibrium amount of BT π -adsorbed through the thiophene ring was probably the species from which HDS actually takes place (via prior hydrogenation to DHBT) on Mo- and Re-based heterogeneous catalysts.^{18c}

Along these lines, our results show that the hydrogenation of BT catalyzed by 1 occurs regiospecifically at the heterocyclic ring whereas the benzene ring is never reduced under these conditions; this can be taken as an indication that this catalysis is related to the structure 4a, and not to 4b. The accumulated catalytic and NMR data, however, are not conclusive, and we have complemented our experimental work with the quantum mechanical calculations described in the next section.

Theoretical Analysis of the Structure of 4. In order to better understand the structure of 4, we have performed a theoretical study of the simplified PH_3 analogues 4', using the semiempirical SCF-CNDO/2 method. In our discussion we first describe the free BT ligand and the metal fragment represented by $\text{Rh}(\text{PH}_3)_2^+$ (5'); then we analyze the interaction between these two fragments, and the structures resulting from the various possible coordination modes.

Calculations on BT. Figure 3 shows the charges on the atoms in BT. The atom numbering in this figure is used throughout this paper. The frontier orbitals are shown in the extremes of Figure 4. The occupied MO's are particularly important because this molecule acts as an electron donor from its π -system to the metal.⁵ The HOMO (5a'') is highly localized on the S atom; it has a small bonding C2-C3 contribution and does not contain any contribution from C4 or C5. This orbital corresponds essentially to what is commonly viewed as the S π lone pair. Slightly lower in energy, we find 4a'' which contains S-C2, C2-C3, and C7-C8 bonding interactions.

Calculations on $\text{Rh}(\text{PH}_3)_2^+$ (5'). This C_{2v} fragment was constructed by use of the structural parameters previously reported by us for 3 (Rh-P = 2.254 Å and P-Rh-P = 96.9°).¹⁴ Other geometrical parameters were P-H = 1.44 Å and Ru-P-H = 118°. The center of Figure 4 shows the frontier orbitals of 5'. The Rh atom presents a charge of +0.367 and the orbital population described in Table 3. In the following discussion it is desirable to refer the symmetry of these orbitals to the yz plane, since this plane will bisect the thiophene or benzene ring when they coordinate. The a_1 and b_1 orbitals are symmetric with respect to this plane, while a_2 and b_2 are antisymmetric.

The LUMO is 3a₁, containing significant contributions from the Rh 5s (49%), 5p_z (27%) and 4d_{z²} orbitals (10%). Higher but very close in energy we find 2b₁ (5p_y, 56%;

(18) (a) Wang, C.-M. J.; Angelici, R. J. *Organometallics* 1990, 9, 1770. (b) Hockett, S. C.; Angelici, R. J. *Organometallics* 1988, 7, 1491. (c) Hockett, S. C.; Angelici, R. J.; Ekman, M. E.; Schrader, G. L. *J. Catal.* 1988, 113, 36.

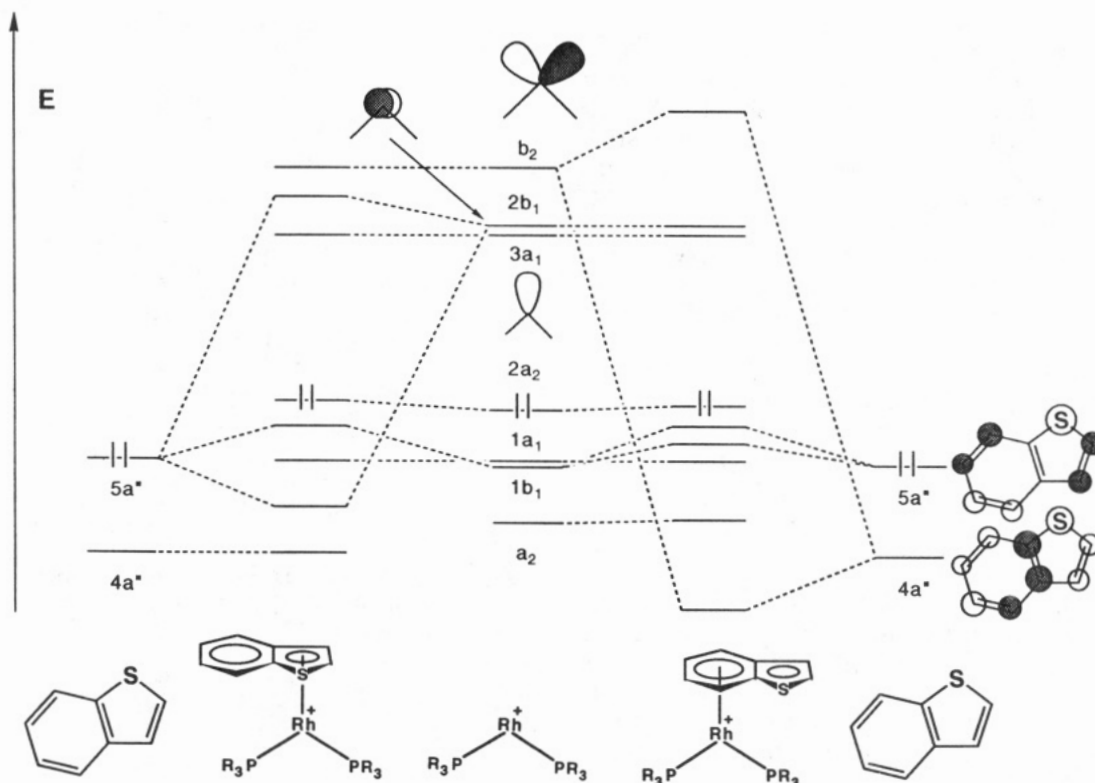


Figure 4. Frontier orbitals of BT and $[\text{Rh}(\text{PH}_3)_2]^+$ and principal orbital interactions involved in the formation of $[(\eta^5\text{-BT})\text{-Rh}(\text{PH}_3)_2]^+$ and $[(\eta^6\text{-BT})\text{Rh}(\text{PH}_3)_2]^+$.

Table 3. Coordination Energies^a and Electronic Populations on the Rh Atom of Complexes 3'–6'

complex	5'	4a'	4b'	3'	6'
CE ^a		−281.8	−277.8	−293.3	−269.1
Rh	+0.367	−0.382	−0.341	−0.431	−0.317
Rh(5s)	0.572	0.612	0.580	0.629	0.594
Rh(5p _x)	0.364	0.447	0.445	0.460	0.451
Rh(5p _y)	0.096	0.510	0.503	0.530	0.470
Rh(5p _z)	0.187	0.382	0.368	0.387	0.363
Rh(4d _z)	1.643	1.678	1.721	1.672	1.712
Rh(4d _{xz})	0.202	0.443	0.477	0.451	0.431
Rh(4d _{yz})	1.809	1.606	1.549	1.612	1.582
Rh(4d _{x²−y²)}	1.871	1.838	1.837	1.831	1.847
Rh(4d _{xy})	1.889	1.866	1.861	1.861	1.860

^a CE (in kcal/mol). For definition, see ref 19.

4d_{yz}, 7%) and b₂ (5p_x, 25%; 4d_{xz}, 50%). We note that another set of calculations performed by Harris for 5' reports b₂ as the LUMO, but the details of this work have not been disclosed.^{4c} In any case, the analysis of the orbital interactions in both the η^5 - and η^6 -bonding modes does not change significantly if the $\text{Rh}(\text{PH}_3)_2$ fragment is taken from our calculations or from those of Harris, since the three important orbitals for these interactions (3a₁, 2b₁, and 2b₂) are very close in energy.

Using simple symmetry arguments, we can expect two principal interactions between BT and the fragment 5': (i) donation from the S π lone pair of BT (5a'') to the 3a₁ and 2b₁ orbitals on 5' (this interaction will obviously be most important in the case of BT coordination through the thiophene ring) and (ii) donation from a delocalized 4a'' orbital to the antisymmetric b₂ orbital, which would be of similar importance for the η^5 (4a') and η^6 (4b') complexes. Let us now analyze these interactions.

Coordination of BT and Related Ligands. The compounds studied in this section are related to the T

derivative 3;¹⁴ in the case of BT we have explored both coordination possibilities using the PH_3 analogues 4a' and 4b'.

The only parameter optimized in this case was the distance from the Rh atom to the mass center of the thiophene ring in 4a' and to the mass center of the benzene moiety in 4b', using in both cases a pseudosymmetry C_{2v} . The structures of the Rh fragment 5' and of BT are maintained constant along the reaction path. Table 3 shows the coordination energies (CE)¹⁹ and the electronic populations on the metal atom of $\text{Rh}(\text{PH}_3)_2$ (5'), $\text{Rh}(\text{PH}_3)_2$ -(η^5 -BT) (4a'), and $\text{Rh}(\text{PH}_3)_2$ -(η^6 -BT) (4b'). For comparison, calculations were also performed on $[\text{Rh}(\eta^5\text{-T})(\text{PH}_3)_2]^+$ (3') and the benzene analogue $[\text{Rh}(\eta^6\text{-benzene})(\text{PH}_3)_2]^+$ (6'); those results are also included in Table 3.

From these data several interesting conclusions can be drawn: (i) the order of stability of the complexes is 3' (−293.3 kcal/mol) > 4a' (−281.8 kcal/mol) > 4b' (−277.8 kcal/mol) > 6' (−269.1 kcal/mol). These energies show that BT coordination through the thiophene ring as in 4a' and through the benzene ring as in 4b' are about equally probable, and therefore we cannot unambiguously distinguish between the η^5 and η^6 modes for BT; our results also indicate that in the complexes containing the isolated ring ligand, η^5 -thiophene seems to bind more strongly (3') than η^6 -benzene to $[\text{Rh}(\text{PH}_3)_2]^+$ (6'). (ii) The charge transfer, as previously reported for Mo–T complexes,⁵ is from BT to the metal fragment; (iii) there is a clear correlation indicating that a higher charge transfer implies a higher coordination energy.

On analyzing Table 3 in combination with Figure 4 we note important changes in 5s, 5p_z, and 5p_y, which are a measure of the 5a''–3a₁–2b₁ interaction. These changes

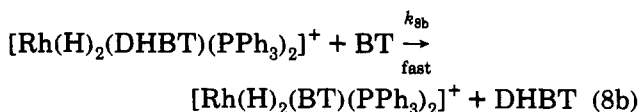
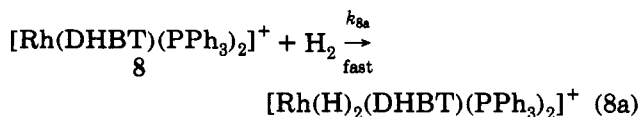
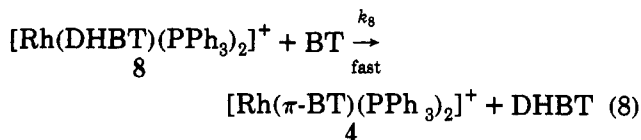
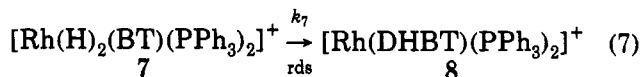
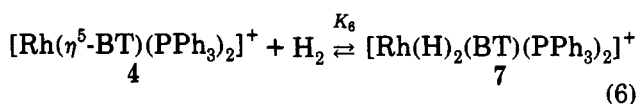
(19) The coordination energy is defined as the total energy in the equilibrium geometry minus the energy of $\text{Rh}(\text{PH}_3)_2^+$ plus the corresponding ligand.

are greater in the η^5 case (**4a'**) than in the η^6 case (**4b'**). On the other hand, the change of $4d_{xz}$, which is related to the $4a''$ - b_2 interaction, is slightly larger for **4b'** than it is for **4a'**. These results are also suggestive that S lone pair donation is the most important factor in the coordination of the thiophene ring, whereas coordination of the benzene ring is controlled by $4a''$ donation.

Although in our calculations the internal structures of the thiophene and benzothiophene ligands were not allowed to relax, another important interaction that becomes evident from our analysis is the one taking place between the occupied $1b_1$ metal orbital ($4d_{yz}$) and an occupied ligand orbital ($2b_1$, $5a''$, and $4a''$ for **3'**, **4a'**, and **4b'**, respectively). This 4-electron two-orbital interactions are highly repulsive and are localized on the Rh-S bond in the cases of **3'** and **4a'** and on the Rh-C bonds on the y -axis for **4b'**. This explains the Rh-S bond elongation which has been experimentally observed for the complex $[\text{Rh}(\eta^5\text{-T})(\text{PPh}_3)_2]^+$ ¹⁴ and predicts similar distortions in the Rh-BT structures.

In conclusion, our theoretical analysis shows that the orbital disposition in the fragment **5'** is adequate for binding to BT in both the η^5 -thiophene fashion and in the alternative η^6 -benzene mode. On the basis of these two possibilities, and taking into account the selectivity observed in our catalytic work, together with previous knowledge on this and closely related subjects we propose that the η^5 -thiophene bonding mode is the most likely one to be directly involved in the catalytic cycle.

Mechanism of the Hydrogenation of Benzo[*b*]-thiophene. On the basis of the discussion presented above, we propose that complex **4**, in which the BT is π -bonded to Rh (probably in an equilibrium mixture of the η^5 and η^6 forms), is an active species directly implicated in the catalysis. This complex reacts with hydrogen to yield a dihydrido species $[\text{Rh}(\text{H})_2(\text{BT})(\text{PPh}_3)_2]^+$ (**7**), according to the equilibrium represented by eq 6. Sub-



sequent hydrogen transfer to produce the intermediate $[\text{Rh}(\text{DHBT})(\text{PPh}_3)_2]^+$ (**8**) is the rate determining step (k_7); the catalytic cycle is completed by rapid displacement of DHBT by a new BT molecule to **8** to regenerate **4**, or

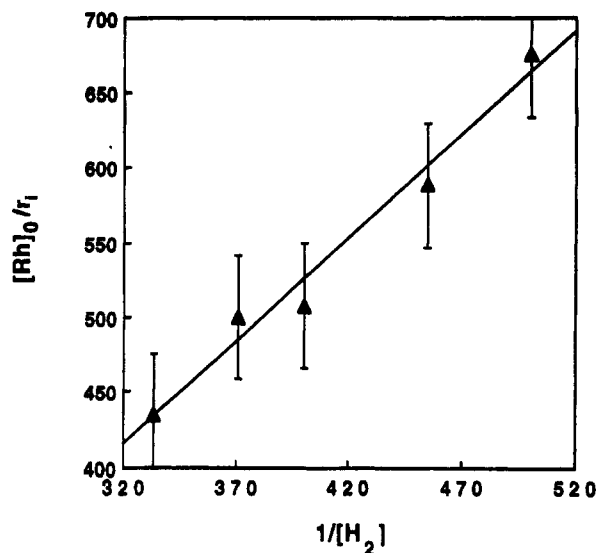


Figure 5. Hydrogenation of benzothiophene to 2,3-dihydrobenzothiophene. Plot of $[\text{Rh}]_0/r_i$ vs $1/[\text{H}_2]$. Conditions are as in Table 1.

alternatively by rapid oxidative addition of H_2 to **8**, followed by displacement of DHBT by BT (eqs 8a and 8b).

According to this mechanism, a rate law can be derived, taking into account that the initial rate of product formation is represented by eq 9.

$$r_i = d[\text{DHBT}]/dt = k_7[\text{7}] \quad (9)$$

Considering the equilibrium in eq 6 and the mass balance for rhodium ($[\text{Rh}]_0 = [\text{4}] + [\text{7}]$), the concentration of **7** may be expressed as in eq 10. Substituting **7** in eq 9

$$[\text{7}] = \frac{K_6[\text{Rh}]_0[\text{H}_2]}{1 + K_6[\text{H}_2]} \quad (10)$$

leads to

$$r_i = \frac{k_7 K_6 [\text{Rh}]_0 [\text{H}_2]}{1 + K_6 [\text{H}_2]} \quad (11)$$

This theoretical rate law is in good accord with our experimental findings, in that it predicts a first order dependence with respect to hydrogen at low concentrations ($K_6[\text{H}_2] \ll 1$) and a tendency toward zero order as the hydrogen concentration is increased ($K_6[\text{H}_2] \approx 1$). This implies that **4** should be the dominant species in the former case, while **7** should be the most abundant intermediate in the latter.

Further, eq 11 can be inverted and reorganized as in eq 12.

$$\frac{[\text{Rh}]_0}{r_i} = \frac{1}{k_7 K_6 [\text{H}_2]} + \frac{1}{k_7} \quad (12)$$

A plot of $[\text{Rh}]_0/r_i$ vs $1/[\text{H}_2]$ yields a straight line (Figure 5) from which the values of K_6 (19.61 M^{-1}) and k_7 ($3.70 \times 10^{-2} \text{ s}^{-1}$) were obtained. At low hydrogen concentrations the rate expression can be simplified to

$$r_i = k_7 K_6 [\text{Rh}]_0 [\text{H}_2] \quad (13)$$

which is identical to the approximate experimentally determined rate law, where $k_{\text{cat}} = k_7 K_6$. This also implies

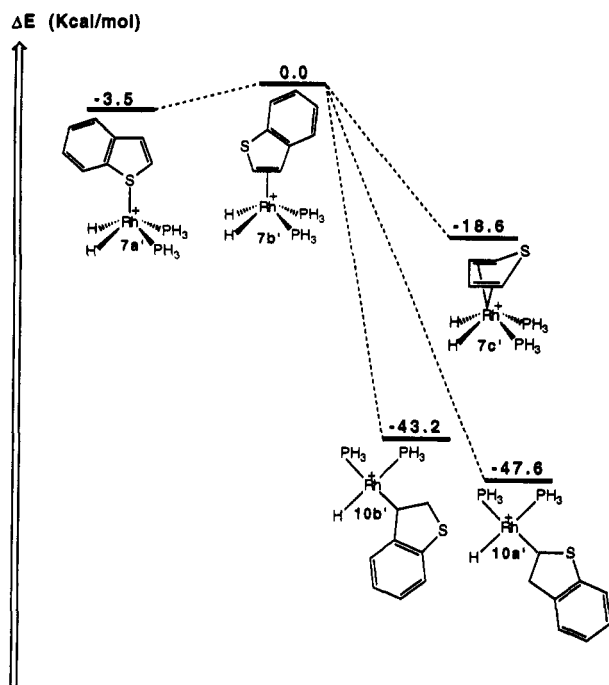


Figure 6. Calculated relative energies of various complexes resulting from the interaction of $[(\eta^5\text{-BT})\text{Rh}(\text{PPh}_3)_2]^+$ with hydrogen.

that the calculated (overall) activation parameters must be dependent on both K_6 and k_7 ; the fact that a linear Arrhenius plot was obtained indicates that both constants vary in the same direction and in similar magnitudes with the reaction temperature over the range studied.

In order to have a better understanding of the details involved in this mechanism, we have complemented our experimental findings with a theoretical (CNDO) analysis of some possible intermediates implicated in the catalytic cycle.

We must note that upon reaction of 4 with H_2 , the BT ligand must change its coordination mode, as otherwise there would be too many electrons around the rhodium atom. Thus we will first discuss the possible structures of the dihydrido intermediate 7. For this purpose, we have calculated a set of structures (see Computational Details) where BT coordinates η^1 (7a'), η^2 (7b'), or η^4 (7c') to a square-based pyramid constituted by the rhodium atom, two hydrides, and two PPh_3 ligands, $[\text{Rh}(\text{H})_2(\text{PPh}_3)_2]^+$ (9'). The relative energies of the various possible intermediates are shown in Figure 6.

We observe that the most stable complex of this series is the 18-electron η^4 species (7c'); about 20 kcal higher we find the η^1 (7a') and the η^2 (7b') structures, which are energetically very close to one another. Additionally, the two possible alkyl species resulting from migration of a hydride to C2 (10a') and to C3 (10b') of BT have been calculated; a large drop in energy is observed in either case, and only a slight preference (4.4 kcal/mol) for migration to the C3 rather than to C2 can be noticed.

Besides the relative energies, it is perhaps more instructing to compare the effect of Rh coordination on the C2–C3 bond order and on the atomic charge of each carbon atom (Table 4), which gives us a measure of the activation of the bond that is being hydrogenated. We note that, as expected, coordination in any fashion lowers the charges of C2 and C3; this effect is larger for the η^2 case (7b') than for the other two modes of bonding of BT. In all three

Table 4. Rh, C2, and C3 Charges and S–C2 and C2–C3 Mulliken Bond Orders (MBO) for Complexes 7a'–7c'

complex	$q(\text{Rh})$	$q(\text{C2})$	$q(\text{C3})$	MBO(C2–C3)
BT		–0.024	+0.024	2.08
7a'	–0.215	+0.052	+0.060	2.04
7b'	–0.183	+0.089	+0.089	1.91
7c'	–0.192	+0.041	+0.078	1.99

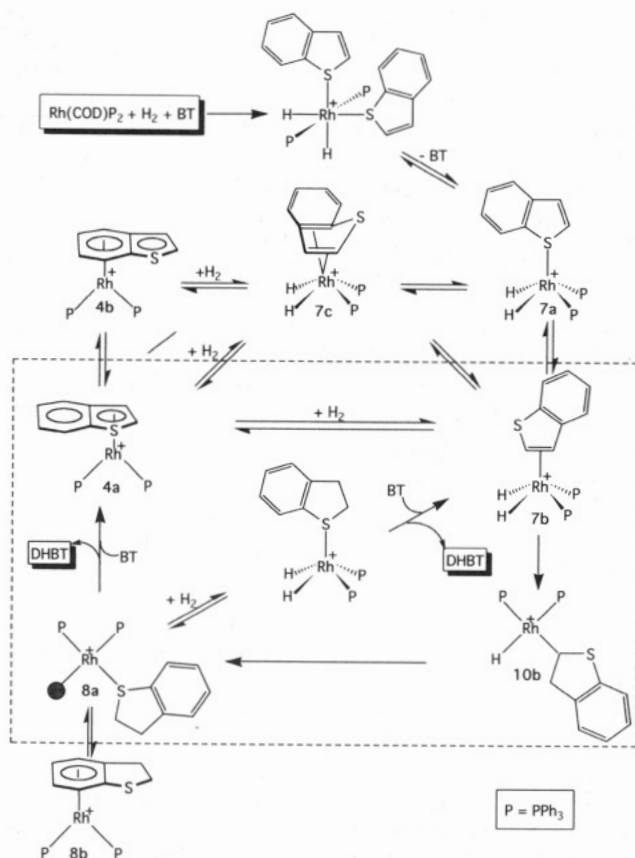
cases, the effect on C2 is very similar to the effect on C3. On this basis alone we could infer that hydride migration should not discriminate between C2 or C3 in any one of the three structures, which is coherent with the small energy difference computed between both alkyl species 10a' and 10b'; however, in the η^1 case, C3 is much further away in space than C2 from the Rh atom, and therefore one would expect a selective migration to the α position, which is not the case. We can take the argument further by noticing that the C2=C3 bond order decreases along the series BT (2.08) > η^1 (7a') (2.04) > η^4 (7c') (1.99) > η^2 (7b') (1.91), which means that the η^2 olefin-like coordination in fact produces a considerably higher activation than η^1 or η^4 .

These combined arguments lead us to the conclusion that the dihydrido species directly participating in the cycle is most probably the 16-electron $[\text{Rh}(\text{H})_2(\eta^2\text{-BT})(\text{PPh}_3)_2]^+$. We mentioned that 1 reacts with H_2 and BT to produce first the 18-electron bis-BT intermediate $[\text{Rh}(\text{H})_2(\eta^1\text{-BT})_2(\text{PPh}_3)_2]^+$ (11) (cf. the stable analogous Ir derivative),¹⁵ which would dissociate one BT ligand in solution to yield 7a and then isomerize into the η^2 form to enter the catalytic cycle as 7b. One could nevertheless conceive an alternative cycle based on 11 and subsequent bis(BT) intermediates; in order to clarify this point, we have also calculated the structures of $[\text{Rh}(\text{H})_2(\eta^1\text{-BT})_2(\text{PPh}_3)_2]^+$ (11a') and the one resulting from shifting one BT from the η^1 - to the η^2 -bonding mode, $[\text{Rh}(\text{H})_2(\eta^1\text{-BT})(\eta^2\text{-BT})(\text{PPh}_3)_2]^+$ (11b'). This latter isomerization is accompanied by a considerable jump in energy (+68.1 kcal/mol), resulting from the large steric congestion caused by the presence of both η^1 and η^2 ligands on the same rhodium atom. On the other hand, dissociation of one BT ligand would require only 39.1 kcal mol^{–1}; the driving force for this dissociation would be the energy gain involved in the subsequent transfer of hydrides to form the corresponding metal–alkyl intermediates. We may thus reasonably rule out a mechanism involving the bis-BT route and keep to our proposed mono-BT intermediates.

Conclusions and Final Remarks

Our experimental findings combined with our theoretical analysis allow us to postulate the catalytic cycle represented in Scheme 1. The species within the dotted lines are the ones we believe to be directly participating in the hydrogenation catalysis. BT initially binds η^1 -S to Rh(III) in 7a and rearranges to the dihydrido η^2 complex 7b. A reversible loss of dihydrogen would produce a η^5 -BT Rh(I) species 4a which may be in equilibrium with the η^6 isomer 4b (outside the cycle); the olefin-like intermediate 7b undergoes selective hydrogenation of the C2=C3 bond to yield a species containing the hydrogenated product, namely $[\text{Rh}(\eta^1\text{-S-DHBT})(\text{PPh}_3)_2]^+$ (8a). This intermediate may also be in equilibrium with its η^6 isomer 8b outside the cycle. Reaction of 8a with a new BT molecule would liberate the product and produce 4a to restart the cycle. Alternatively, 8a could react with H_2 to yield $[\text{Rh}$

Scheme 1. Postulated Mechanism for the Regioselective Hydrogenation of Benzothiophene by Use of $[\text{Rh}(\text{COD})(\text{PPh}_3)_2]\text{PF}_6$ as the Catalyst Precursor



$(\text{H})_2(\eta^1\text{-S-DHBT})(\text{PPh}_3)_2]^+$, followed by displacement of DHBT by $\eta^2\text{-BT}$. In accord with this we have recently observed that the closely related $[\text{Ir}(\text{H})_2(\eta^1\text{-S-BT})_2(\text{PPh}_3)_2]^+$ ^{15a} reacts with hydrogen under mild conditions to generate $[\text{Ir}(\text{H})_2(\eta^1\text{-S-DHBT})_2(\text{PPh}_3)_2]^+$. ^{15b}

This catalytic cycle is closely related to the familiar Rh-catalyzed olefin hydrogenation mechanism and quantitatively accounts for our kinetic results. The outer species do not participate directly in the catalysis, and an accumulation of any one of them would result in loss of activity; they may, however, exist in appreciable concentrations under conditions different from the ones producing the catalysis. All the species postulated in Scheme 1 are justified by either some direct or indirect experimental evidence, or by reasonable theoretical argumentation.

Fish and co-workers^{3f} have also argued in favor of the involvement of the η^2 -bonding mode in the hydrogenation of BT catalyzed by $[\text{Cp}^*\text{Rh}(\text{NCCCH}_3)_3]^{2+}$, on the basis of deuteration experiments. Other workers have further shown the importance of the η^2 coordination in the activation of thiophene. Choi and Angelici^{20a,b} have demonstrated that the complexes $\text{Cp}'(\text{CO})_2\text{Re}(\text{BT})$ ($\text{Cp}' = \text{Cp}, \text{Cp}^*$) easily interconvert by an intramolecular process between the $\eta^1\text{-S}$ - and η^2 -bonded isomers in CDCl_3 solution at room temperature and have pointed out the importance of such equilibria in relation to the hydrogenation of

benzothiophene. Jones and Dong have also discussed the possible involvement of η^2 -bonded thiophene in the mechanisms of C-S activation on Rh centers. $\eta^5\text{-BT}$ adsorption has also been postulated to be responsible for HDS of BT on heterogeneous catalysts.^{18c} These precedents provide further support for our proposal.

Other general features of this catalytic cycle are similar to those involved in the one proposed by Fish^{3f} for $[(\text{C}_5\text{-Me}_5)\text{Rh}(\text{NCMe})_3]^{2+}$ on the basis of chemical and spectroscopic evidence; however, an important difference becomes apparent. Fish and co-workers start with a Rh-(III) precursor and invoke a dicationic intermediate containing Cp^* and one or more H (or D) ligands, besides benzothiophene bonded to the metal; this suggests that in their case Rh has to go through oxidation states higher than 3 at some point in the cycle, which is unusual. In our case we go through the cycle using only Rh(I)/Rh(III) couples formed by standard oxidative addition–reductive elimination processes.

Another interesting point is encountered in the final step proposed for each mechanism. The 12-electron $\text{Cp}^*\text{Rh}^{2+}$ fragment displays a strong affinity for arenes; in the Fish mechanism, the last step involves migration of the hydrogenation substrate toward an 18-electron π -bonded arene form, followed by displacement of $\eta^6\text{-DHBT}$ by $\eta^2\text{-BT}$, which restarts the catalytic cycle. In our case, we can envisage displacement of $\eta^1\text{-S-DHBT}$ from **8a** or of $\eta^6\text{-DHBT}$ from **8b** by $\eta^5\text{-BT}$, or an alternative situation in which oxidative addition of H_2 to **8** precedes displacement of the product by a substrate molecule.

Hydrogenation of BT to DHBT has been proposed as the first step in the heterogeneous hydrodesulfurization of this compound.^{1f,g} The complexity of the real catalysts and the severity of the heterogeneous reaction conditions make a detailed mechanistic study of the hydrogenation step extremely difficult; therefore, homogeneous modeling of such hydrogenations may indeed provide new insights into the difficult problem of HDS catalysis. We believe that this piece of work illustrates a very good approach combining kinetic, chemical, and theoretical evidence to reach a deeper understanding of a homogeneous catalytic reaction. The mechanism deduced from these studies is also likely to be closely related to the pathways through which BT is converted to DHBT by use of heterogeneous catalysts. In further papers we will apply this methodology to other important metal-mediated organic transformations.

Experimental Section

Instrumentation and Materials. Rhodium(III) trichloride hydrate (Alfa), ammonium hexafluorophosphate (Aldrich), and triphenylphosphine (Aldrich) were used without further purification. Benzothiophene (Aldrich) was purified by recrystallization from ethanol/water. All the solvents were dried and distilled under N_2 . The complex $[\text{Rh}(\text{COD})(\text{PPh}_3)_2]\text{PF}_6$ was prepared according to published procedures.²¹ NMR spectra were obtained by using a Bruker AM-300 instrument.

Hydrogenation Experiments. The hydrogenation reactions were carried out using the apparatus previously described by us.^{12b} In a typical experiment a solution of $[\text{Rh}(\text{COD})(\text{PPh}_3)_2]\text{PF}_6$ and BT in 2-methoxyethanol was placed in a glass reactor fitted with a reflux condenser kept at 0°C . The reactor was sealed with Apiezon wax to a high vacuum line, and the solution was carefully degassed by three freeze–pump–thaw cycles;

(20) (a) Choi, M.-G.; Robertson, M. J.; Angelici, R. J. *J. Am. Chem. Soc.* **1991**, *113*, 4005. (b) Choi, M.-G.; Angelici, R. J. *Organometallics* **1992**, *11*, 3328. (c) Jones, W. D.; Dong, L. *J. Am. Chem. Soc.* **1991**, *113*, 559.

(21) Giordano, G.; Crabtree, R. H. *Inorg. Synth.* **1979**, *19*, 218.

hydrogen was admitted at this point to the desired pressure, an electric oven preheated to the required temperature was placed around the reactor, and magnetic stirring was immediately commenced. The reactions were followed by measuring the hydrogen pressure drop as a function of time. Each reaction was repeated at least twice to ensure reproducibility of the results. In order to use the initial rates method the conversion of reactants in the catalytic reactions was generally (although not necessarily) kept below 10% (ca. 5–20 turnovers). The data were plotted as molar concentration of the product as a function of time, yielding straight lines; initial hydrogenation rates were obtained from the corresponding slopes. All the straight lines were fitted by conventional linear regression programs to $r^2 > 0.98$. The hydrogen concentration in solution under the reaction conditions was calculated according to published solubility data.²²

Computational Details. All calculations were performed with the semiempirical SCF-CNDO/2 method.²³ The computer program used is based on the QCPE-290 program described by Rinaldi.²⁴ For the Rh atom the effective ionization energies were also derived from atomic data²⁵ as $EI(5s) = 7.60$ eV, $EI(5p) = 4.19$ eV and $EI(4d) = 8.71$ eV. The basis set for Rh consisted of single- ζ Slater orbitals with exponents 2.822 (4d) and 1.482 (5s and 5p). These exponents were taken from INDO calculations in which they extensively provided satisfactory results concerning energies and geometries.²⁶ In the process we developed parameters suitable for the calculation of molecular properties in organometallic complexes containing Rh. β parameters for Rh,

$\beta(4d) = 12.606$ eV and $\beta(5s) = \beta(5p) = 1.000$ eV, were calculated by fitting the experimental²⁷ Rh–C bond distance (1.614 Å) and dissociation energy (140 kcal/mol). The Rh parameters used in this study are not fully optimized, but they are not expected to be significantly different from the final set. Here, we are more interested in a qualitative study similar to Hoffmann's work for other transition metal complexes. Standard parameters²³ were used for H, C, P, and S; the 3d orbitals were included for the P and S atoms, because it is known that they play an important role in the electronic properties of metal–phosphine²⁸ and metal–sulfur²⁹ compounds. Due to limited computing resources, we have imposed some constraints in the study of the reaction pathways. Some geometrical parameters which are not essential for the reaction have been frozen. Symmetry has been fully considered whenever possible.

The structures **7a'**, **7b'**, and **7c'** were optimized on an idealized $Rh(H)_2(PH_3)_2$ square planar arrangement. Some geometrical parameters of this structure are: $d(H-H) = 1.3$ Å, $d(Rh-H_2) = 1.5$ Å; $\angle(P-Rh-P) = 140^\circ$, $\angle(P-Rh-P-H_2) = 122^\circ$. In the case of **7a'** and **7b'** the calculations were performed without altering the geometry of the BT molecule, while for **7c'** the thiophene structure was optimized.

Acknowledgment. We thank Fundayacucho for a Graduate Fellowship (to L.R.), and Dr. F. Ruette (IVIC) and Prof. B. R. James (Vancouver) for interesting discussions and very useful suggestions.

OM9307186

(22) Brunner, E. *Ber. Bunsen-Ges. Phys. Chem.* **1979**, *83*, 715.

(23) Pople, J. A.; Beveridge, D. L. *Approximate Molecular Orbital Theory*; McGraw-Hill: New York, 1970.

(24) Rinaldi, D. *Comput. Chem.* **1976**, *1*, 109.

(25) van der Lugt, W. T. A. M. *Int. J. Quantum Chem.* **1972**, *6*, 859.

(26) (a) Anderson, W. P.; Cundari, T. R.; Zerner, M. C. *Int. J. Quant. Chem.* **1991**, *39*, 31. (b) Anderson, W. P.; Cundari, T. R.; Drago, R. S.; Zerner, M. C. *Inorg. Chem.* **1990**, *29*, 1.

(27) Rosen, B., Ed. *Selected Constants, Spectroscopic Data Relative to Diatomic Molecules*; Pergamon Press: New York, 1970; p 334.

(28) (a) Orpen, A. G.; Connelly, N. G. *Organometallics* **1990**, *9*, 1206. (b) Xiao, S.-X.; Troglor, W. C.; Ellis, D. E.; Berkovitch-Yellin, Z. *J. Am. Chem. Soc.* **1983**, *105*, 7033.

(29) (a) Naray-Szabo, P.; Peterson, M. R. *J. Mol. Struct.* **1981**, *85*, 249. (b) Friedman, P.; Allen, L. C. *Int. J. Quantum Chem.* **1986**, *29*, 1503.